

$^{13}\text{C}(\gamma, p)$ cross section

D. Zubanov, R. A. Sutton, and M. N. Thompson

School of Physics, University of Melbourne, Parkville, Victoria, 3052, Australia

J. W. Jury

*School of Physics, University of Melbourne, Parkville, Victoria, 3052, Australia
and Department of Physics, Trent University, Peterborough, Ontario, Canada K9J 7B8*

(Received 3 January 1983)

A high resolution measurement of the $^{13}\text{C}(\gamma, p)$ cross section is presented from threshold to 28 MeV. In combination with the known $^{13}\text{C}(\gamma, n)$ cross section an estimate of the total absorption cross section is obtained and compared with current theoretical predictions. An estimate of the distribution of the isospin components in the giant dipole resonance shows that isospin splitting and the relative $T_<$ and $T_>$ strengths are in agreement with predictions.

NUCLEAR REACTIONS $^{13}\text{C}(\gamma, p)$, $E_\gamma = 17.5\text{--}28.0$ MeV; measured beta activation yield with bremsstrahlung, deduced cross section, integrated cross section, comparison with theory, isospin GDR components deduced.

I. INTRODUCTION

Several photonuclear studies of light nuclei consisting of a $4N$ core plus a single valence nucleon or hole have been published within the past few years.¹⁻³ To some extent these results suggest that a weak coupling model can be used with standard shell model techniques to describe the reported cross sections. Certainly in the cases of ^{17}O and ^{29}Si , the presence of a pygmy resonance at least, is consistent with this model.

The nucleus ^{13}C is a prime candidate for study, having one neutron outside a ^{12}C core. Indeed, measurements of the photoneutron cross section^{4,5} reveal considerable absorption strength forming a pygmy resonance below the region of the giant dipole resonance (GDR). Consistent with the weak coupling model these low-lying transitions will proceed mainly via excitation of the valence neutron to form $T = \frac{1}{2}$ states in ^{13}C . It would be expected that no such pygmy resonance would be observed in the photoproton channel unless more complex multiparticle-multihole configurations are being formed.

The ground state isospin of ^{13}C is $T = \frac{1}{2}$ so that electric dipole ($E1$) excitation will populate $T = \frac{1}{2}$ and $T = \frac{3}{2}$ (the so-called $T_<$ and $T_>$) states in the GDR. According to Akyüz and Fallieros⁶ these two isospin components of the GDR are split so that

their median energies are separated by $\Delta E = U(T_0 + 1)/A$ MeV where T_0 is the ground state isospin and U is the symmetry energy. Confirmation of this effect is certainly found in medium mass nuclei.⁷ In the case of ^{13}C this isospin splitting has a particularly notable effect, in that many single particle states are pushed down from the GDR and are clearly visible in the $^{13}\text{C}(\gamma, n_0)$ cross section measured by Woodworth *et al.*⁸ and the $^{13}\text{C}(\gamma, n)$ results of Jury *et al.*⁵ In addition, these latter results indicate a significant resonance on the rising edge of the GDR at 20.7 MeV. This resonance has been recently interpreted⁹ as a primary doorway state interfering with a 3p-2h secondary doorway state which has a negligible photon width. The present measurement by virtue of its comparable resolution provides additional information which can clarify the isospin nature of the GDR, and of this state in particular.

Many theoretical calculations have been made for the photoabsorption cross section in ^{13}C . Being a relatively simple nucleus, most of these are shell model calculations with different residual interactions.¹⁰⁻¹⁴ A new approach on the basis of the direct-semidirect model by Dietrich and Kerman¹⁵ is also available. All these calculations make different predictions (sometimes significantly different) for the photoabsorption cross section of ^{13}C ; thus it is important to obtain a good measurement of this for comparison.

Currently there is no measurement of the photo-

absorption cross section, although this could be estimated if reliable high resolution measurements existed for the various decay channels. Such measurements are available for the $^{13}\text{C}(\gamma,sn)$ reaction⁵ and for the photoneutron cross section to the ground state of ^{12}C (Refs. 8–16) and to higher residual states.¹⁷ However, the available measurements of the $^{13}\text{C}(\gamma,p)$ reaction have relatively poor resolution. Two^{4–18} were made at a time when yield curve unfolding techniques lacked the sophistication subsequently developed¹⁹; the other²⁰ was a proton spectrum measurement with relatively poor resolution and subject to decay-mode assumptions in deriving the cross section. The measurement reported here has resolution comparable to that of the measurement of Jury *et al.*,⁵ and when combined with this, will allow a better comparison with the theoretical calculations.

A study of the comparison of the integrated electric dipole photoabsorption cross section for nuclei in the $1p$ shell is summarized in a recent paper by Jury *et al.*² There is some evidence that the values for the self-conjugate nuclei are systematically smaller than those for their non-self-conjugate neighbors. Data for $^{17}\text{O}(\gamma,p)$ are not available and those currently available for $^{13}\text{C}(\gamma,p)$ are, as mentioned above, subject to some uncertainty.

This paper presents a high resolution measurement of the $^{13}\text{C}(\gamma,p)$ cross section and discusses the implications following from these data, particularly as they can be used to obtain the photoabsorption cross section.

II. EXPERIMENTAL DETAILS

The cross section for the $^{13}\text{C}(\gamma,p)^{12}\text{B}$ reaction was derived from the yield of induced β^- activity from ^{12}B , measured as a function of bremsstrahlung energy. The ^{12}B nucleus decays by β^- emission with a half-life of 20.4 ms. Transitions to the ground state of ^{12}C with a maximum β^- energy of 13.37 MeV account for 97.1% of the decay, and a further $(1.29 \pm 0.05)\%$ (Ref. 21) is accounted for by decay to the 4.439 MeV state in ^{12}C . The high end-point en-

ergy of the β^- spectrum allowed detection of the beta particles with NaI detectors in the experimental arrangement described below.

The target consisted of approximately 75 g of ^{13}C -enriched graphite as detailed in Table I. The composite sample consisting of two pressed graphite discs and graphite powder in two thin-walled aluminum containers measured 37 mm in diameter by 97 mm long. This sample was placed in a bremsstrahlung beam from the University of Melbourne betatron, which was collimated to a diameter of 25 mm when measured at the center of the sample. The photon flux of this beam was measured by a thin-walled transmission chamber placed upstream of the sample, and which was intercalibrated against a replica P2 ionization chamber.²²

Two NaI detectors were placed on one side of the sample and another on the opposite side. The detectors had their front faces close to the sample and were in a horizontal plane perpendicular to the beam direction. Shielding was provided by 0.15 m of steel stacked around the detectors. This arrangement permitted the detection of the induced β^- activity between the 2 μs duration 50 Hz repetition rate bremsstrahlung beam from the betatron.

In order to maintain the photomultiplier tube (PMT) stability and to protect the detectors from damage due to the intense beam scattered by the sample, it proved necessary to gate the PMT's off during the beam burst. Further gain stability was obtained by including an analog stabilizer in the electronic circuitry immediately before the lower level discriminator, which was set to pass signals corresponding to electron energies greater than 2.6 MeV.

A total of 11 independent yield curves were measured at bremsstrahlung tip energies ranging from 17 MeV to 29 MeV in 100 keV intervals. Each yield curve took approximately 6 h to complete and was done under computer control of beam parameters. Curves were taken in alternating order of increasing or decreasing beam energy. This procedure tends to average out short term drifts in the stability of the

TABLE I. ^{13}C sample characteristics.

Sample source	Isotopic purity (%)	Mass (g)	Thickness (g/cm^2)
Triangle Universities Nuclear Laboratory	99	14.35	1.30
Lawrence Livermore National Laboratory	98.6	14.87	1.35
Trent University and University of Toronto	94.6	32.4	3.0
University of Melbourne	85.9	13.52	1.22

electronics. In addition, a standard reference yield point was taken after each 10 points as a check of the reproducibility. In practice, no need for corrections was indicated by these data.

A separate set of three yield curves was measured with the sample replaced by an equivalent mass of ^{12}C graphite together with two empty sample containers. This background yield was a small fraction of the sample-in yield; typical values as a fraction of the sample-in yield were 10% at 19 MeV, 2% at 24 MeV, and 1% at 28 MeV. In addition, a set of three yield curves was measured from 17 to 22 MeV in energy intervals of 50 keV. These higher-resolution data were taken in an effort to resolve fine structure in the region below the GDR. It is an accepted advantage of the yield curve method that it has proven very reliable in resolving fine structure in this energy region.¹⁹⁻²³

As will be discussed below, it was necessary to record separately the data from the detectors on either side of the sample and take weighted averages to provide two sets of yield curves (one for detectors on either side of the sample) corrected for background. One set ranged from 17 to 29 MeV in 100 keV intervals and the other from 17 to 22 MeV in 50 keV intervals.

An important aberration of the Melbourne University betatron is that at electron energies above 23 MeV, there is an energy-dependent lateral shift in the direction of emission of the bremsstrahlung beam. This effect is small, so that at the sample a maximum shift of 3 mm in the location of the most intense region of the beam is observed. However, a significant effect occurred in this experiment since the detected electrons have emerged from a thick sample.

Because of ionization effects in the sample, the energy loss of some electrons in the β^- spectrum is such that the energy deposited in the detector crystal is insufficient to allow them to be registered above the detection threshold. As the beam intensity centroid moves to one side, some of these electrons pass through less of the sample and reach the detector with a higher energy, thereby registering above the detection threshold.

An essentially inverse effect is observed in the opposing detection system. In consequence, the ratio of yields in the two detector systems changes in a bremsstrahlung-energy-dependent manner. However, because the specific ionization of the electrons near the detection threshold of 2.6 MeV is essentially energy independent, the effect in the opposing detectors is almost complementary. Thus, to first order the unperturbed yield curve can be obtained from the weighted average of the two detectors.

Another experiment, incorporating a second set of

detectors placed above and below the sample, was done to check for any second order beam shift effects. The averaged yields of the detectors in the vertical plane (where the positional shift of the bremsstrahlung beam was negligible) indicated that no further corrections to the averaged yield curves of the horizontal detectors were required.

Although detection of the β^- decay from the residual ^{12}B nuclei provided a relatively efficient means of determining the relative yield curve for the $^{13}\text{C}(\gamma,p)$ reaction, it was not feasible to determine the absolute efficiency of the electron detection system. However, a small percentage ($1.29 \pm 0.05\%$) (Ref. 21) of the β^- decay populates the first excited state of ^{12}C (4.439 MeV). The use of a NaI detector of known efficiency to measure the yield of 4.439 MeV γ rays at a particular bremsstrahlung energy provided a means of normalizing the relative yield scale of the carefully determined β^- -activity yield curves referred to above.

An auxiliary normalization experiment using a

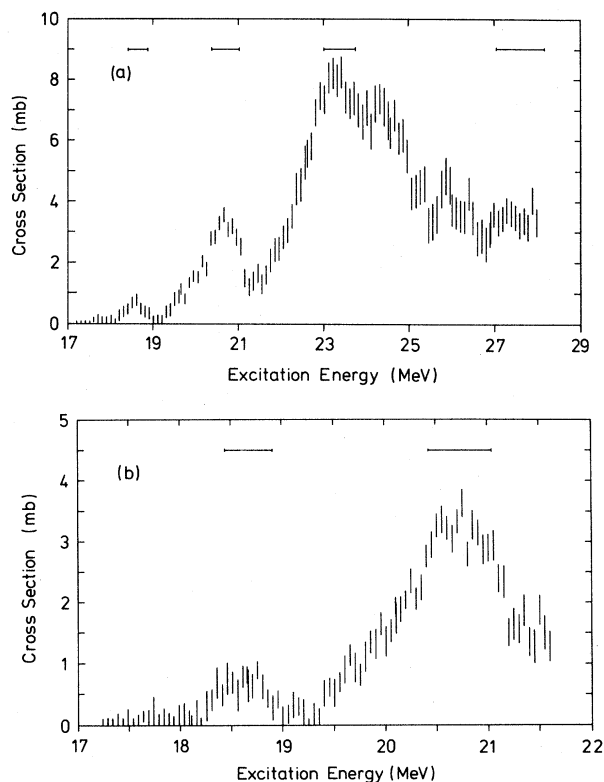


FIG. 1. (a) The $^{13}\text{C}(\gamma,p)^{12}\text{B}$ cross section derived from yield data measured in 100-keV intervals. The error bars represent statistical uncertainties only; there is a systematic uncertainty of 13%. Horizontal bars indicate the approximate energy resolution. (b) The $^{13}\text{C}(\gamma,p)^{12}\text{B}$ cross section derived from yield data measured in 50-keV intervals. Other details are as for (a).

single well shielded and absolutely calibrated 0.10 m diam \times 0.13 m NaI detector measured 4.439 MeV γ rays from a ^{13}C sample with a known geometry. Approximately 20 mm of aluminum was placed in front of the detector to remove the underlying background of β particles, allowing a clean spectrum of the 4.439 MeV γ ray to be obtained. The yield of γ rays was measured at bremsstrahlung end-point energies of 24 and 28 MeV.

The efficiency of the γ -ray detection system for 4.439 MeV γ rays was determined by using a coincidence technique first published by Wapstra.²⁴ The reaction $^{11}\text{B}(p,\gamma)$ was used to populate the 16.11-MeV state in ^{12}C which decays to the 4.439-MeV state and then to the ^{12}C ground state. By using two detectors, so that coincidences could be taken between the 11.67 MeV γ ray in one detector with the 4.439 MeV γ ray in the detector to be calibrated, an absolute photopeak efficiency was obtained for the 4.439 MeV γ ray.

III. ANALYSIS AND RESULTS

After correcting the raw yield curve data for the effects of the betatron beam shift and background, two yield curves (one in 100 keV intervals from 17 to 29 MeV and another in 50 keV intervals from 17 to 22 MeV) were available for further analysis.

The cross sections were unfolded from these yield curves using the variable bin Penfold-Leiss method developed in this laboratory.²⁹ Figure 1(a) shows the cross section deduced from the 100 keV interval yield curve and Fig. 1(b) shows the lower energy region derived from the yield curve measured in 50 keV intervals. The error bars represent statistical uncertainties only; there is a systematic uncertainty of about 13%.

The main strength occurs above 22 MeV, al-

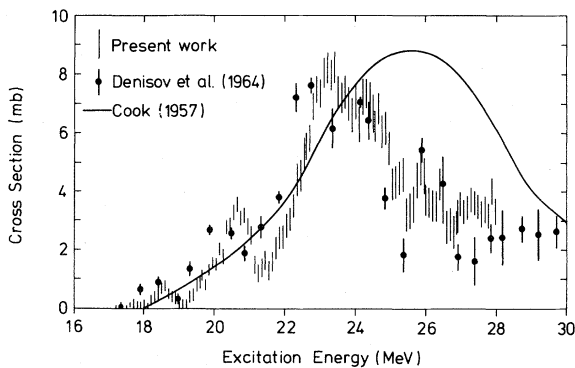


FIG. 2. Comparison of several measurements of the $^{13}\text{C}(\gamma,p)^{12}\text{B}$ cross section. Data points are the present results, the dots are the results of Denisov *et al.* (Ref. 18), and the full line represents the results of Cook (Ref. 4).

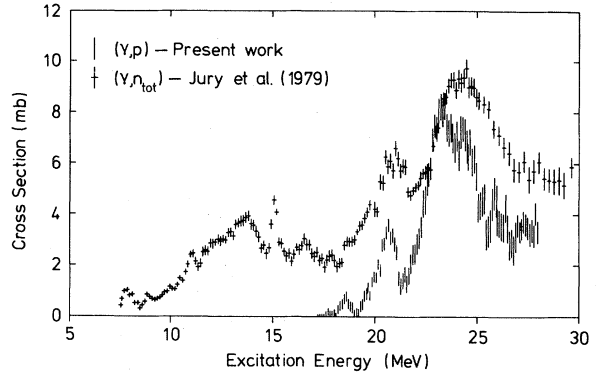


FIG. 3. The $^{13}\text{C}(\gamma,p)^{12}\text{B}$ cross section reported here together with the $^{13}\text{C}(\gamma,n)^{12}\text{C}$ cross section of Ref. 5.

though considerable strength continues above this structure up to 28 MeV, the limit of the present measurement, and includes evidence of a peak at about 26 MeV. On the rising side of this resonance at about 22 MeV there is some evidence for at least one smaller broad resonance. The other significant feature of the cross section is a well-defined shoulder resonance at 20.7 MeV. Figure 1(b) reveals the detail in the cross section from threshold (17.5 MeV) to 21.5 MeV, and identifies a clear resonance at 18.6 MeV. There appears to be some evidence for underlying strength near 19.7 on the rising side of the 20.7 MeV resonance.

IV. DISCUSSION

A. Comparison with experiment

Previous low resolution measurements of the $^{13}\text{C}(\gamma,p)$ cross section showed considerable disagreement in both cross-section magnitude and structure. For example, the very early measurement by Cook⁴ showed no evidence of the peak at 20.7 MeV, although this was evident in the $^{13}\text{C}(\gamma,n)$ cross section reported in the same paper.

Of the two previous measurements by Denisov *et al.*¹⁸ and Kosiek *et al.*²⁰ the former also used a yield curve technique based on counting the induced β^- activity of ^{12}B . Comparison of the present data with the results of Denisov *et al.* shows good agreement. The resonances seen in the present data agree more closely with the recent photoneutron measurement from Livermore.⁵ Because the $^{13}\text{C}(\gamma,p)$ cross section reported by Kosiek *et al.*²⁰ is derived from a measurement of the proton spectrum at 90° , it does not extend down to the region of the peak near 21 MeV. In addition, because the cross section is derived on the assumption of ground-state proton emission only, which Patrick *et al.*¹⁷ have shown to be not strictly valid, it is not surprising that a de-

tailed comparison of these data with the present results would not be fruitful. Figure 2 shows the present data together with those of Denisov *et al.* and Cook.

Figure 3 shows the $^{13}\text{C}(\gamma, p)$ cross section reported here, together with the $^{13}\text{C}(\gamma, n)$ measurement of Jury *et al.*⁵ from which the sum incorporated into Fig. 4 was obtained. When taken in conjunction with the inelastic electron scattering measurements of Bergstrom *et al.*,²⁵ the resonances listed in Table II can be inferred.

B. Integrated cross sections

It should be noted that the cross section represents only the single proton strength from the $^{13}\text{C}(\gamma, p)$ reaction: Proton strength in the $^{13}\text{C}(\gamma, np)^{11}\text{B}$ reaction is not measured here but is included in the $^{13}\text{C}(\gamma, sn)$ measurement of Ref. 5. The integrated photoproton cross section from threshold (17.5 MeV) to 28 MeV is 36 ± 5 MeV mb. This is to be compared with a value of 42 MeV mb estimated from the results of Denisov *et al.*¹⁸ over the same energy region. A total integrated strength predicted by the semiclassical electric dipole Thomas-Reiche-Kuhn (TRK) sum rule is 193.8 MeV mb for ^{13}C . The fraction of this value exhausted by the photoproton channel up to 28 MeV is $(19 \pm 3)\%$. Compared with this, the photoneutron cross section

$$\sigma(\gamma, n) + \sigma(\gamma, np) + \sigma(\gamma, an) + \sigma(\gamma, 2n)$$

integrated up to 28 MeV is 84.9 MeV mb, which is 44% of the TRK sum rule. Together these photonuclear reactions in ^{13}C , integrated to 28 MeV, exhaust 63% of the $E1$ sum rule. This value is higher

than for its self-conjugate neighbor, ^{12}C , and is consistent with the systematic trends in $1p$ shell nuclei summarized by Jury *et al.*²

C. Comparison with theoretical predictions

In order to evaluate the various theoretical calculations for the photoabsorption process in ^{13}C it is necessary to know the total absorption cross section. This can be approximated by summing the present $^{13}\text{C}(\gamma, p)$ data and the equivalent $^{13}\text{C}(\gamma, sn)$ cross section from Livermore.⁵ The contributions of other decay modes (d , α , γ , etc.) are assumed to be small. No measurements of these cross sections for ^{13}C have been reported, but since in the case of ^{12}C the photo-alpha cross section constitutes less than 5% (Ref. 26) of the absorption cross section, it seems likely that the contribution of such reactions to the ^{13}C photoabsorption cross section will also be small.

The present total photonuclear cross section is compared with recent theoretical calculations in Fig. 4, where the calculated photoabsorption results have been normalized in the GDR region. The calculation of Albert *et al.*¹³ was performed using a $2p-1h$ shell model with harmonic oscillator basis states and allows both $E1$ and $M1$ absorption. Calculations with two different residual forces were done; a modified zero range potential with a Soper mixture of exchange forces [Fig. 4(a)] and a separable Tabakin interaction [Fig. 4(b)], where each level has been assigned an arbitrary width of 2 MeV. The calculation using the Soper interaction is in better agreement with the measured location and strength distribution in the GDR region, as shown in Fig. 4(a). This was also observed to be the case for ^{17}O .¹

TABLE II. Comparison of observed resonances in ^{13}C for $17.5 < E_x < 28.0$ MeV. The parentheses indicate resonances that are not well established.

Present experiment	Denisov <i>et al.</i> (Ref. 18)	Jury <i>et al.</i> (Ref. 5)	Bergstrom <i>et al.</i> (Ref. 25)
$^{13}\text{C}(\gamma, p)$ (MeV)	$^{13}\text{C}(\gamma, p)$ (MeV)	$^{13}\text{C}(\gamma, n)$ (MeV)	$^{13}\text{C}(e, e'p)$ (MeV)
			18.3
18.6	18.5	(18.7)	18.7
(19.7)		(19.8)	19.3
20.7	20.0		20.1
(22)		(22.2)	20.5
23.5	23.5		21.3
24.5		24.4	22.2
(26)	26.0		24.7
			25.5
			27.3

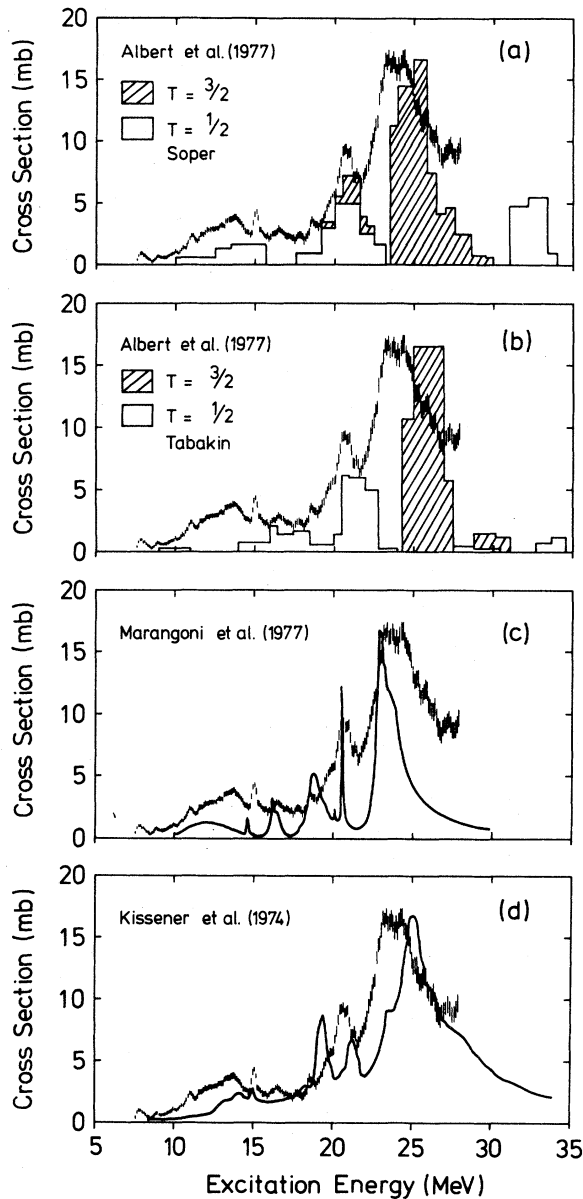


FIG. 4. Comparison between the total photoabsorption cross section of ^{13}C and several theoretical calculations: (a) that of Albert *et al.* (Ref. 13) using a residual interaction with a Soper mixture; (b) that of Albert *et al.* (Ref. 13) using a Tabakin force; (c) that of Marangoni *et al.* (Ref. 11); (d) that of Kissener *et al.* (Ref. 10).

However, the calculations do not account adequately for the presence of the pygmy resonance in either ^{13}C or for ^{17}O . In contrast, for the case of the ^{15}N photoneutron cross section, the Tabakin interaction gives better agreement with the results of Jury *et al.*² It appears as though the theoretical calculation of the cross section using a 1p-2h model is satisfactory when the Tabakin potential is used, but

2p-1h nuclei are described better by a Soper mixture. The failure of these theoretical calculations to account for the experimental results for all three odd- A nuclei (^{13}C , ^{15}N , and ^{17}O) using the same residual interaction illustrates deficiencies of this simplified treatment and shows the need for a more general approach or the use of a more sophisticated shell model method incorporating more realistic residual interactions.

Marangoni *et al.*¹¹ have analyzed the dipole photo-reactions of ^{13}C in the 2p-1h approximation of the continuum shell model. Agreement was found to be reasonable for the $^{13}\text{C}(\gamma, n)$ cross section. Figure 4(c) compares the total absorption cross section with the calculation. There is clearly an underestimate of the GDR width.

Kissener *et al.*¹⁰ analyzed the decay of the GDR by using the bound-state shell model and R -matrix theory. The model used a phenomenological interaction determined from a fit to $A = 13$ and 14 nuclear energy levels, nonspurious bound state wave functions without isospin mixing, and R -matrix formulation for particle widths. Figure 4(d) shows the comparison with the total absorption cross section. With due allowance for the apparent energy shift the agreement is satisfactory. The gross structure of the ^{13}C absorption cross section is well reproduced by all the calculations.

The particle-hole calculations of Albert *et al.* and Kissener *et al.* predict that the pygmy region and the peak near 20 MeV are mainly due to $T = \frac{1}{2}$ ($T_{<}$) states, while the region above about 21 MeV is composed predominantly of $T = \frac{3}{2}$ ($T_{>}$) states. Marangoni *et al.*, in a discrete calculation additional to that referred to above, calculate the isospin components of ^{13}C taking into account all the configurations of $1\hbar\omega$ excitation. This calculation predicts that the pygmy resonance and the peak near 20 MeV are $T_{<}$ states, and the giant resonance peak at 23.5 MeV is $T_{>}$; however, it gives no indication of $T_{<}$ strength in the 21–25 MeV region. This is in contrast to Kissener *et al.* and Albert *et al.* who predict significant $T_{<}$ strength in the GDR region and above. All these calculations predict that roughly $\frac{1}{3}$ of the dipole strength is carried by $T_{<}$ states and $\frac{2}{3}$ by $T_{>}$. It is interesting to see what the results of the present measurement, when taken in conjunction with similar resolution photoneutron data for both the total and ground-state reactions, can reveal about the isospin strength distribution.

D. Isospin considerations

Electric dipole absorption by a non-self-conjugate nucleus with ground state isospin of T_0 will populate states with isospin T_0 and $T_0 + 1$. [In self-

conjugate nuclei ($T_0=0$), only states with isospin $T=1$ are populated.] These dipole states form the GDR and are generally referred to as the $T_<$ and $T_>$ GDR components, respectively. Expressions for the relative strengths of these two components have been developed by O'Connell^{27,28} and Goulard and Fallieros²⁹ and can be expressed in terms of the ratio of the energy weighted integrated cross sections of the $T_<$ and $T_>$ components, i.e.,

$$\frac{\sigma_{>}^{-1}}{\sigma_{<}^{-1}},$$

where

$$\sigma^{-1} \equiv \int_0^\infty \sigma/E dE.$$

For the particular case of ^{13}C where $T_0 = \frac{1}{2}$, the ratio is estimated to be 1.22 using the O'Connell sum rule²⁸ and to be 1.36 according to Goulard and Fallieros.²⁹ In addition, as mentioned in the Introduction, for the case of ^{13}C the centroids of these two isospin components should be separated by 6.9 MeV if the symmetry energy U is 60 MeV, as is assumed by Akyüz and Fallieros.⁶ It is of interest to see if the isospin components of the photoabsorption cross section for ^{13}C can be identified, and if the separations of the isospin strengths compare favorably with the predictions.

Figure 5 shows the relevant level and kinematic data for the $^{13}\text{C}(\gamma, n)$ and $^{13}\text{C}(\gamma, p)$ reactions. Regions in ^{13}C are shown to represent schematically $T_<$ and $T_>$ states in the GDR. From these states, proton and neutron decays are shown to the residual states in ^{12}B and ^{12}C , respectively. Also shown are the relative Clebsch-Gordan coupling coefficients between the GDR states of isospin $\frac{1}{2}$ and $\frac{3}{2}$ to the residual states of isospin 0 and 1 (decays to $T=2$ residual states are energetically forbidden). The lowest $T = \frac{3}{2}$ state occurring at an excitation energy of 15.11 MeV ($\frac{3}{2}^-$) is strongly populated, and decays by neutron emission (proton decay being energetically forbidden). Its population and decay are contrary to angular momentum and isospin selection rules and indicate a degree of mixing with nearby $T = \frac{1}{2}$ negative parity states. The main $T = \frac{3}{2}$ strength starts at about 18.5 MeV if we use the listed³⁰ analog states in ^{13}B as a guide, and continues upward. So it is clear that cross section strength above about 18.5 MeV in ^{13}C can be due to both $T_<$ and $T_>$ states.

Decay of a particular dipole state by neutron or proton emission depends essentially on two characteristics: whether it is $T = \frac{1}{2}$ or $\frac{3}{2}$ (since the isospin coupling coefficients differ for each decay mode), and the number of residual states available. In addition, for proton decay the effect of the Coulomb

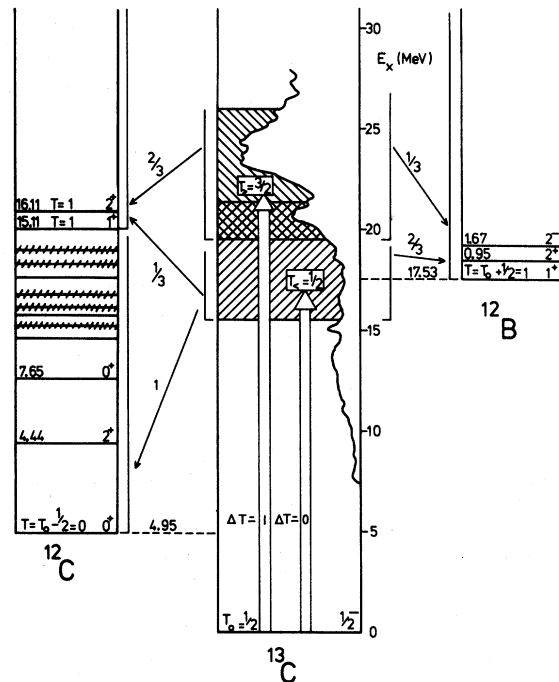


FIG. 5. The kinematic data for the ^{13}C photoreactions. Some of the relevant nuclear states are shown plus the Clebsch-Gordan coefficients which couple the $T = \frac{1}{2}$ and $T = \frac{3}{2}$ GDR isospin states in ^{13}C to the $T=0$ and $T=1$ residuals in ^{12}C and ^{12}B .

barrier must be considered. Consequently, for a state of particular isospin the ratio $\sigma(\gamma, p)/\sigma(\gamma, n)$ can be estimated and when compared with this ratio as determined experimentally, might reveal the isospin composition of the GDR as a function of excitation energy. Figure 6 shows the ratio $\sigma(\gamma, p)/\sigma(\gamma, n)$ determined from the present measurement and that of Jury *et al.*⁵

Up to an excitation energy of 17.5 MeV (the photoproton threshold) only photoneutron emission is

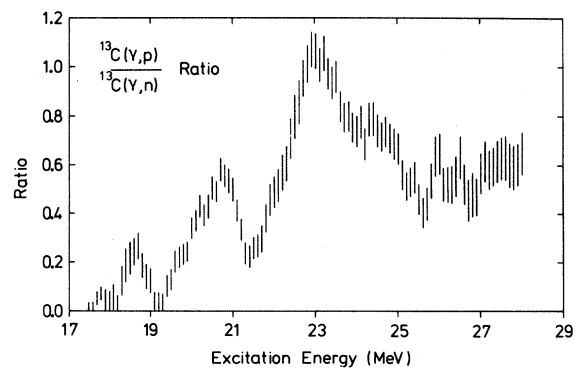


FIG. 6. The ratio of the $^{13}\text{C}(\gamma, p)$ cross section (present data) to the $^{13}\text{C}(\gamma, n)$ cross section (Ref. 5).

possible and this of course represents entirely the decay of $T = \frac{1}{2}$ dipole states. The first clear feature of the photoproton cross section is the resonance at 18.6 MeV. Despite the fact that this is only 1.1 MeV above the (γ, p) threshold and there is a Coulomb barrier of 2.8 MeV, it is clearly evident in the photoproton cross section, and more significantly in the ratio $\sigma(\gamma, p)/\sigma(\gamma, n)$ of Fig. 6. These observations can be interpreted to indicate that the ^{13}C states involved are largely $T = \frac{3}{2}$ in nature, as described below. For a state at 18.6 MeV with isospin $T = \frac{1}{2}$, neutron decay is favored over proton decay by a factor of $\frac{3}{2}$ by virtue of Clebsch-Gordan coupling coefficients between the $T = \frac{1}{2}$ state in ^{13}C and the $T=0$ and $T=1$ states in ^{12}C and ^{12}B , respectively. Additionally, two states in the daughter ^{12}C are available for neutron emission (see Ref. 17), compared with only one at this energy, for proton emission; and of course the neutrons suffer no Coulomb inhibition. This situation would produce a ratio $\sigma(\gamma, p)/\sigma(\gamma, n)$ close to zero. On the other hand, a $T = \frac{3}{2}$ state at 18.6 MeV in ^{13}C is forbidden to decay to any state in ^{12}C , and hence despite the Coulomb barrier, the decay of such a state must proceed via proton emission and would lead to a ratio significantly above zero.

The location of $T_{>}$ strength in this energy region is consistent with predictions of Kissener *et al.*¹⁰ who place the lowest $T_{>}$ strength at about 18 MeV. Also the analogs of a group of low-lying states in ^{13}B should cluster in this region. Several of the ^{13}C states near 18.6 MeV have been identified as having isospin of $\frac{3}{2}$ (see Ref. 30).

The next major feature at 20.7 MeV is known from the measured $^{13}\text{C}(\gamma, n_0)$ cross section⁸ to have significant $T_{<}$ strength. The ratio shown in Fig. 6 does lend some weight to the conclusion that there is also $T_{>}$ strength present. A $T_{<}$ state at this energy would have access to the Coulomb uninhibited decay by proton emission to the ground state of ^{12}B and attenuated decay to the first excited state. Such decays are weighted by a factor of $\frac{2}{3}$ compared with neutron decay to the two lowest states in ^{12}C which, as for the decay of the 18.6 MeV resonance, are energetically favored. The ratio $\sigma(\gamma, p)/\sigma(\gamma, n)$ would thus be expected to be small for a $T_{<}$ state. On the other hand, from a $T_{>}$ state at this energy, neutron decay to the lower energy states of ^{12}C is forbidden, and decay to the first $T=1$ residual at 15.11 MeV is only just energetically possible. Hence, the observed increase in the $\sigma(\gamma, p)/\sigma(\gamma, n)$ ratio at this energy is consistent with the presence of some $T_{>}$ strength in this resonance. There is convincing evidence of this admixture from measurements of the $^{13}\text{C}(\gamma, n)$ and $^{13}\text{C}(\gamma, n_0)$ cross sections by Jury *et al.*⁵ and Wood-

worth *et al.*⁸ taken in conjunction with the work of Patrick *et al.*¹⁷ In the region of the 20.7 MeV resonance the $^{13}\text{C}(\gamma, n_0)$ and $^{13}\text{C}(\gamma, n_1)$ cross section amplitudes are about 2.5 mb and 1.3 mb,⁸ respectively. According to Patrick *et al.* no other $T=0$ states in ^{12}C are populated. Thus, 2.7 mb from this resonance is due to decays to the $T=1$ residual state at 15.11 MeV in ^{12}C since the $^{13}\text{C}(\gamma, sn)$ strength is about 6.5 mb.⁵ The isospin coupling coefficients favor decays of $T_{<}$ in ^{13}C to $T=0$ states in ^{12}C by a factor of 3 over decays to $T=1$ states in ^{12}C . This means that the strength to the $T=1$ state in ^{12}C is made up of 1.3 mb due to decays from $T_{<}$ states and about 1.4 mb from $T_{>}$. Because of the isospin coupling coefficients from a $T_{>}$ state, and the fact that the ground state of ^{12}B (accessible to proton decay) is the analog of the 15.11 MeV state in ^{12}C , we estimate that approximately 0.7 mb of the measured 4 mb photoproton cross section at 20.7 MeV derives from $T_{>}$ states in ^{13}C .

On the basis that the $T_{>}$ strength is dominant, the ratio $\sigma(\gamma, p)/\sigma(\gamma, n)$ should be simply that of the Clebsch-Gordan coupling coefficients, or $\frac{1}{2}$. This deduction is consistent with the value of the ratio above 25 MeV excitation, as shown in Fig. 6.

Further interpretation of the detailed structure of the $\sigma(\gamma, p)/\sigma(\gamma, n)$ data of Fig. 6 is not possible without additional experimental information such as the photoproton cross sections to the ground and excited states of ^{12}B . However, the assumption of a weak coupling model to describe ^{13}C does allow a second, novel, and informative analysis of the isospin nature of the GDR of ^{13}C .

It is generally agreed that the ^{13}C nucleus can be pictured to a first order as a ^{12}C core with a single valence neutron in the $p_{1/2}$ orbit. On this basis the total photonuclear cross section of ^{13}C can be interpreted as that of the ^{12}C core plus that due to the presence of the valence neutron.

For the case of ^{12}C (a self-conjugate nucleus), the nuclear photoabsorption cross section is entirely $T=1$ ($T_{>}$) in nature, whereas that of ^{13}C contains both $T_{>}$ and $T_{<}$ components. On the basis of the model it is assumed that the $T_{>}$ component in the ^{13}C GDR is essentially due to the ^{12}C core and hence can be approximated by the ^{12}C photoabsorption cross section. Thus an estimate of the $T_{<}$ strength in the ^{13}C GDR can be obtained by subtracting the ^{12}C absorption cross section (i.e., the $T_{>}$ strength) from that of ^{13}C . The result of this in Fig. 7 shows the remnant $T_{<}$ strength and the $T_{>}$ strength. In this analysis the total absorption cross section for ^{12}C that was used is that reported by Ahrens *et al.*³¹ appropriately normalized.

A normalizing factor of 0.78 was applied to the ^{12}C photoabsorption cross section, since in the re-

gion of the GDR it is larger than that of ^{13}C , so that on subtraction there would be a negative remainder in the region of the GDR. This would imply, again, on the basis of the model, that the $T_>$ integrated cross section for ^{13}C is less than that of ^{12}C , which is not unexpected as T_0 changes from zero for ^{12}C to $\frac{1}{2}$ for ^{13}C . However, experimental uncertainties could also contribute to this difference. In addition, the ^{12}C data were shifted up in energy by 0.8 MeV to account for the expected energy shift of a $T = \frac{3}{2}$ GDR in ^{13}C compared with a $T = 1$ GDR in ^{12}C .

The remnant $T_<$ strength in the ^{13}C photoabsorption cross section, as shown in Fig. 7, lies mainly below 22 MeV; however, there is non-negligible strength at higher energies, for example at 25 MeV. Kissener *et al.*¹⁰ and Albert *et al.*¹³ predict significant $T_<$ strength at high energies. Such a distribution of $T_<$ strength is also indicated by the work of Patrick *et al.*¹⁷ and Jury *et al.*⁵ In particular, the Livermore group⁵ report the average emitted neutron energy over the region of the GDR. This energy shows an anomalous rise from a value of about 3 MeV at an excitation energy of 25 MeV to a value of 11 MeV at 28 MeV excitation. This was interpreted as evidence of significant neutron decay to the ground and low-lying states of ^{12}C . From this it was inferred that there was significant $T_<$ strength at this excitation.

The results of this exercise are that values of $\int_0^{28} \sigma/E dE$ can be obtained for the isospin components of the ^{13}C photoabsorption cross section. The values are $\sigma_<^{-1} = 2.31$ mb and $\sigma_>^{-1} = 3.54$ mb, thus giving a ratio $\sigma_>^{-1}/\sigma_<^{-1}$ of 1.5 which compares favorably with the ratio predicted by

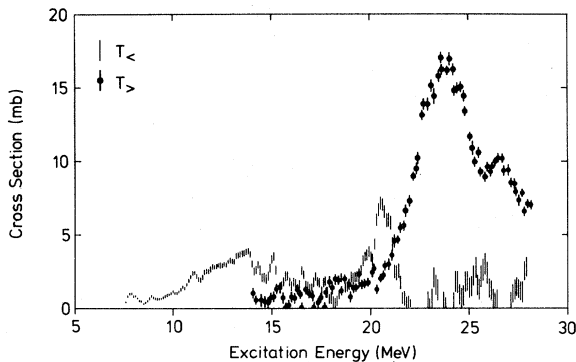


FIG. 7. The resolved $T_<$ and $T_>$ components of the ^{13}C photonuclear cross section. The $T_>$ strength is essentially the total absorption cross section measured by Ahrens *et al.* (Ref. 31) for ^{12}C , after normalization and a small energy shift (see text). The $T_<$ strength is the result of subtraction of this ^{12}C ($T_>$) cross section from that of ^{13}C .

O'Connell²⁷ of 1.22 and Goulard and Fallieros²⁹ of 1.36.

The integrated cross section for the now deduced $T_<$ and $T_>$ components of the ^{13}C photonuclear cross section are 36 MeV mb and 83 MeV mb, respectively, with an uncertainty of approximately 15%. This agrees with the rough estimate that $\frac{1}{3}$ of the absorption strength is carried by $T_<$ states and $\frac{2}{3}$ by $T_>$. The centroid energies for $T_<$ and $T_>$ components are 17.0 MeV and 23.8 MeV, respectively, thus giving an energy separation of 6.8 MeV. This compares well with the value of 6.9 MeV calculated from the expression $\Delta E = U(T_0 + 1)/A$ from Ref. 6, where $U = 60$ MeV.

It can now be seen that the effect of removing the isospin degeneracy from the GDR states of ^{12}C by the addition of the valence neutron is to split the dipole states so that the $T_>$ centroid energy moves higher up by about 0.8 MeV and the $T_<$ centroid energy moves lower by 6.0 MeV, consistent with the predictions of Ref. 6.

V. CONCLUSIONS

The high resolution measurement of the $^{13}\text{C}(\gamma, p)$ cross section presented here provides a value for the integrated cross section to 28 MeV of 36 ± 5 MeV mb.

When considered together with measurements of the photoneutron channel, it allows some conclusions to be made regarding the structure and magnitude of the total photoabsorption cross section and the distribution of the $T_<$ and $T_>$ isospin strength in the GDR. In particular, it is concluded that below about 18 MeV the cross section is dominated by transitions involving $T_<$ states. The resonance at 18.6 MeV appears to have a significant $T_>$ component, as does the larger resonance at 20.7 MeV where we estimate that about 2 mb of the total 10.0 mb strength is due to $T_>$ states.

A splitting of the two isospin components of the ^{13}C GDR of 6.8 MeV is observed, and this is consistent with the predictions of Akyüz and Fallieros.⁶ Both the cross section and the distribution of isospin strength imply that the calculation by Albert *et al.*¹³ using a Soper potential is better than that employing the Tabakin interaction. The calculations of Kissener *et al.*¹⁰ and Marangoni *et al.*¹¹ also predict the gross structure of the absorption cross section and it is difficult to conclude which calculation provides the most realistic approach to the photonuclear reaction process in ^{13}C .

ACKNOWLEDGMENTS

One of us (J.W.J.) wishes to thank the University of Melbourne for a research fellowship held during

the performance of this work. The authors are also indebted to the Lawrence Livermore National Laboratory and the Triangle Universities Nuclear Labo-

ratory for leading samples of enriched ^{13}C . This work was supported in part by a grant from the Australian Research Grant Committee.

- ¹J. W. Jury, B. L. Berman, D. D. Faul, P. Meyer, and J. G. Woodworth, *Phys. Rev. C* **21**, 503 (1980).
- ²J. W. Jury, B. L. Berman, J. G. Woodworth, M. N. Thompson, R. E. Pywell, and K. G. McNeill, *Phys. Rev. C* **26**, 777 (1982).
- ³R. E. Pywell, B. L. Berman, P. Kean, and M. N. Thompson, *Nucl. Phys.* **A369**, 141 (1981).
- ⁴B. C. Cook, *Phys. Rev.* **106**, 300 (1957).
- ⁵J. W. Jury, B. L. Berman, D. D. Faul, P. Meyer, K. G. McNeill, and J. G. Woodworth, *Phys. Rev. C* **19**, 1684 (1979).
- ⁶R. Ö. Akyüz and S. Fallieros, *Phys. Rev. Lett.* **27**, 1016 (1971).
- ⁷M. N. Thompson, *Lecture Notes in Physics* **92**, edited by B. A. Robson (Springer, Berlin, 1978), p. 208.
- ⁸J. G. Woodworth, K. G. McNeill, J. W. Jury, P. D. Georgopoulos, and R. G. Johnson, *Can. J. Phys.* **55**, 1704 (1977).
- ⁹J. G. Woodworth, R. A. August, N. R. Roberson, D. R. Tilley, H. R. Weller, H. Yao, and J. W. Jury, *Bull. Am. Phys. Soc.* **27**, 709 (1982).
- ¹⁰H. R. Kissener, A. Aswad, R. A. Eramzhian, and H. U. Jäger, *Nucl. Phys.* **A219**, 601 (1974).
- ¹¹M. Marangoni, P. L. Ottaviani, and A. M. Saruis, *Phys. Lett.* **49B**, 253 (1974); *Nucl. Phys.* **A277**, 239 (1977).
- ¹²J. Höhn, H. W. Barz, and I. Rotter, *Nucl. Phys.* **A330**, 109 (1979).
- ¹³D. J. Albert, A. Nagl, J. George, R. F. Wagner, and H. Überall, *Phys. Rev. C* **16**, 503 (1977).
- ¹⁴M. N. Kirchbach, Joint Institute of Nuclear Research, Report E4-81-283, Dubna, 1981 (unpublished).
- ¹⁵F. S. Dietrich and A. K. Kerman, *Phys. Rev. Lett.* **43**, 114 (1979).
- ¹⁶J. G. Woodworth, K. G. McNeill, J. W. Jury, P. D. Georgopoulos, and R. G. Johnson, *Nucl. Phys.* **A327**, 53 (1979).
- ¹⁷B. H. Patrick, E. M. Bowey, E. J. Winhold, J. M. Reid, and E. G. Muirhead, *J. Phys. G* **1**, 874 (1975).
- ¹⁸V. P. Denisov, A. V. Kulikov, and L. A. Kul'chitskii, *Zh. Eksp. Teor. Fiz.* **46**, 1488 (1964) [*Sov. Phys.—JETP* **19**, 1007 (1964)].
- ¹⁹E. Bramanis, T. K. Deague, R. S. Hicks, R. J. Hughes, E. G. Muirhead, R. H. Sambell, and R. J. J. Stewart, *Nucl. Instrum. Methods* **100**, 59 (1972).
- ²⁰R. Kosiek, K. Schlüpmann, H. W. Siebert, and R. Wendling, *Z. Phys.* **179**, 9 (1964).
- ²¹F. Ajzenberg-Selove, *Nucl. Phys.* **A248**, 1 (1975).
- ²²J. S. Pruitt and S. R. Domen, *NBS Monograph*, Vol. 48, 1962.
- ²³R. E. Pywell, M. N. Thompson, and B. L. Berman, *Nucl. Instrum. Methods* **178**, 149 (1980).
- ²⁴*Alpha-Beta-Gamma Spectroscopy*, edited by K. Siegbahn (North-Holland, Amsterdam, 1965) Vol. 1, p. 539.
- ²⁵J. C. Bergstrom, H. Crannell, F. J. Kline, J. T. O'Brien, J. W. Lightbody, and S. P. Fivozinsky, *Phys. Rev. C* **4**, 1514 (1971).
- ²⁶M. E. Toms, *Nucl. Phys.* **50**, 561 (1964).
- ²⁷James O'Connell, *Phys. Rev. Lett.* **22**, 1314 (1969).
- ²⁸E. Hayward, B. F. Gibson, and J. S. O'Connell, *Phys. Rev. C* **5**, 846 (1972).
- ²⁹B. Goulard and S. Fallieros, *Can. J. Phys.* **45**, 3221 (1967).
- ³⁰F. Ajzenberg-Selove, *Nucl. Phys.* **A152**, 1 (1970).
- ³¹J. Ahrens, H. Borchert, K. H. Czock, H. B. Eppler, H. Gimm, H. Gundrum, M. Kröning, P. Riehn, G. Sita Ram, A. Zieger, and B. Ziegler, *Nucl. Phys.* **A251**, 479 (1975).